Granular Matter (2012) 14:277–282
DOI 10.1007/s10035-012-0332-5

ORIGINAL PAPER

Statistical-mechanical characteristics of dense planar granular systems

Rebecca Hihinashvili · Raphael Blumenfeld

Received: 20 August 2011 / Published online: 22 February 2012

Abstract We demonstrate the use of a structural and statistical characterisation method on two types of planar disc packs. One is a very dense pack of mean coordination number 5.20 and the other of mean coordination number 4.0. Except for constraining the mean coordination number in the latter one, the different pack types were constructed by the same deposition process and had the same disc size distribution, for a fair statistical comparison. We show that the two types converge to limit statistics and that these limit statistics are different. We analyse the limit statistics and compare between both types of packs, demonstrating that the differences are directly related to the difference in the mean coordination numbers. We then find quantitatively the difference between the (inverse) compactivities of the two pack types: $\frac{1}{X_{5.2}} - \frac{1}{X_4} = 1.5 \pm 0.05$. This explicit result supports strongly the validity of Edwards approach and underpins it as a useful tool to characterise granular systems quantitatively. In particular, it also paves the way to quantify the elusive compactivity.

Keywords Granular material · Structural characterisation · Compactivity · Quadron

R. Hihinashvili
ESE, Imperial College, London, SW7 2AZ, UK
e-mail: rhihinas@imperial.ac.uk

R. Blumenfeld
ESE and ISP, Imperial College, London, SW7 2AZ, UK

R. Blumenfeld (✉)
Cavendish Laboratory, Cambridge, CB3 0HE, UK
e-mail: rbb11@cam.ac.uk

1 Introduction

A key to modelling granular matter is a useful characterisation of the grain-scale structure. In particular, this is essential as a step to derivation of structure-property relations. Such a characterisation should: (i) describe the grain-scale structure quantitatively and (ii) enable large-scale structural characterisation. A method providing both has been suggested in [1–3]. The structure is quantified via a particular tessellation of the granular space and a description of the shape of every volume element by a structure tensor. These elements, called quadrons, are quadrilaterals in two dimensions (2D) and octahedra in three dimensions (3D). In a sense, the quadrons are the elementary 'quasi-particles' in the system, as will become clear below. A brief review of the method in 2D is given below and the 3D version is detailed in [3,4]. For many-particle systems, it is convenient to use an entropy-based statistical mechanical formalism [5–8], based on a volume partition function

$$Z_v = \int e^{-\frac{\mathcal{W}(\{\eta\})}{X}} \Theta(\{\eta\}) d^{N_{\mathrm{DOF}}}\{\eta\}. \tag{1}$$

Here $\Theta(\{\eta\})$ is a product of δ-functions that constrain all possible configurations to a prescribed ensemble, $\mathcal{W}$ is a volume function that sums over all the possible volumes that the quadrons can realise, $\{\eta\}$ are all the structural degrees of freedom (DOF), and X is the compactivity – a measure of the fluctuations in the realisations that is the analogue of the temperature. The DOF are the independent variables that describe the structures of all members of the ensemble. We consider a canonical ensemble of volumes, whose members have N grains and the same mean number of force-carrying contacts $\bar{z} = \sum_g z_g/N$.

This formalism makes it possible to determine expectation values of structural properties, based on *all* possible

configurations. This is to be contrasted with phenomenological approaches where statistics are determined from measurements of a finite number of samples under the assumption that they are typical. As in conventional statistical mechanics, one assumes that, all else being equal, a configuration i of grains occurs with a probability proportional to a Boltzmann-like factor $e^{-V_i/X}$, where V_i is its volume. From (1) we can determine the expectation value of *any* structural property A

$$\langle A\rangle = \frac{1}{Z_v}\int A(\{\eta\})e^{-\frac{\mathcal{W}(\{\eta\})}{X}}\Theta(\{\eta\})d^{N_{\rm DOF}}\{\eta\} \tag{2}$$

Note that expectation values integrate over small-scale degrees of freedom to yield large-scale structural properties, in effect comprising upscaling, or coarse-graining, of structural features. As in thermal systems, this formalism leads to the following relations: $X \equiv \partial\langle V\rangle/\partial S$, where S is the entropy – the logarithm of the number of possible configurations; $\langle V\rangle = -\partial\ln(Z_v)/\partial(1/X)$; and $\langle V^2\rangle - \langle V\rangle^2 = \partial^2\ln(Z_v)/\partial(1/X)^2$.

For the approach to be useful, it was essential to identify the DOF and their number $N_{\rm DOF}$. In the ensemble described above, $N_{\rm DOF} = N\bar{z}$ in 2D assemblies [1] and for 3D tetrahedral (foam-like) structures $N_{\rm DOF} = 3N\left(2-\frac{N_c}{N}\right)$, where N_c is the number of cells [4].

Much research focused in recent years on loosely connected packs due to their importance to the understanding of granular materials near the jamming transition [9–22]. Here we focus on denser systems both because of their theoretical significance and their relevance to many applications, where compactification is a key issue. Moreover, since the dense regime corresponds to low compactivity, we expect that this regime should play as important a role for granular physics as low temperature physics does to physics.

In this paper we apply this approach to dense packs of polydisperse discs in 2D. In Sect. 2 we review briefly the structural quantification method and the construction of a volume function. In Sect. 3 we detail the numerical protocol to construct dense packs of polydisperse discs. We analyse the pack statistics and apply the statistical mechanical formalism in Sect. 4. We show that the algorithm used to construct dense packs leads to limit statistics above a certain pack size and we study the limit distributions of disc sizes, of quadron volumes and of the DOF. We compute the difference between the inverse compactivities of two different types of disc packs. In Sect. 5 we summarise our findings, draw conclusions and outline future work.

[1] It should be noted that there are small corrections to this value due to boundary effects and due to grains with $z_g = 2$.

2 Quantifying the grain-structure: a brief review

A convenient quantitative description of granular structures, proposed in [1–3], is based on tessellation of the pack into specific volume elements and quantifying each element by a structure tensor. First, the contacts of every grain, g, are connected by vectors that circulate it clockwise (Fig. 1), making polygons around the grains and the cells. Each vector is indexed by the grain g and cell c that share it, $\mathbf{r}^{cg}$. Dual to every $\mathbf{r}^{cg}$ is a vector $\mathbf{R}^{cg}$ extending from the centroid of g (the mean position vector of the contact points around g) to the centroid of cell c. These two vectors make the diagonals of a quadrilateral, named quadron [3], which we index, for brevity, by q: $\mathbf{r}^{cg} \to \mathbf{r}^q$ and $\mathbf{R}^{cg} \to \mathbf{R}^q$. A quadron's volume, V^q, includes parts of grain and cell volumes. There are $N\bar{z}$ quadrons and they tessellate the total pack volume

$$\mathcal{W} = \sum_{q=1}^{N\bar{z}} V^q \tag{3}$$

The volume function suggests the quadrons as the natural 'quasi-particles' of the description. Conveniently, the number of quadrons equals $N_{\rm DOF}$ [3].

The quadron structure is quantified unambiguously by $C^q \equiv \mathbf{r}^q \otimes \mathbf{R}^q$. The deviation of $\mathrm{Tr}\{C^q\} = \mathbf{r}^q \cdot \mathbf{R}^q$ from zero measures the deviation of the quadron shape from a perfect kite and the anti-symmetric part of C^q measures its volume, $V^q = \frac{1}{2}|r_x^q R_y^q - r_y^q R_x^q|$.

This description improves over Voronoi-based tessellations: (i) it is based on the actual force-carrying contacts, providing direct information on the contact network; (ii) all

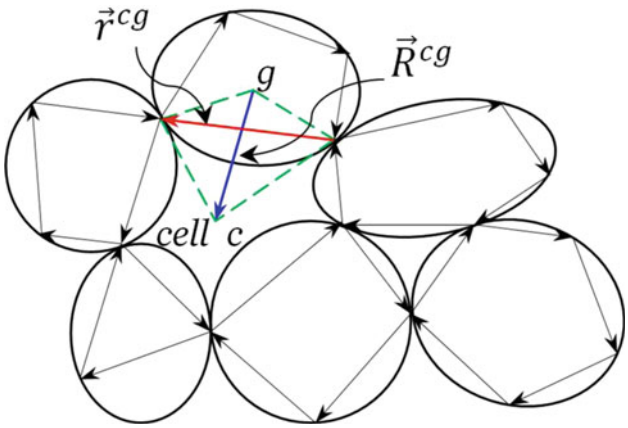

Fig. 1 Quantifying the local structure in 2D granular packs. The intergranular contact points are joined by vectors $\mathbf{r}^{cg}$ to form z_g-edge polygons inside grains and z_c-edge polygons around cells. From the centroid of grain g we extend a vector $\mathbf{R}^{cg}$ to the centroid of a neighbour cell c. The vectors $\mathbf{r}^{cg}$ and $\mathbf{R}^{cg}$ make the diagonals of a quadrilateral (*dashed line*), called quadron. The quadrons tessellate the plane and are the elementary volumes of the system. They are also the 'quasi-particles' for the purpose of the statistical mechanical formalism

the volume elements are quadrilaterals, allowing us to quantify their structures unambiguously.

Not only does this description provide an exact expression for $\mathcal{W}$ in (1), but it also makes possible exact identification of the DOF [3,4]. The latter is based on the following considerations: (i) there are $N\bar{z}$ quadrons; (ii) a quadron volume is determined by $\mathbf{r}^q$ and $\mathbf{R}^q$; (iii) the $\mathbf{R}$-vectors can be expressed as linear combinations of the $\mathbf{r}$'s; (iv) only half of the $\mathbf{r}$ vectors are independent due to the loops that they form. Taken together, these give that $N_{\mathrm{DOF}} = N\bar{z}$. From (iii) we also see that $\mathcal{W}$ can be written in a quadratic form and hence

$$Z_v = \int e^{-\frac{1}{X}\sum_{q,q'=1}^{N\bar{z}/2} a_{ij}^{qq'} r_i^q r_j^{q'}} \Pi_{q=1}^{N\bar{z}/2} dr_x^q dr_y^q \tag{4}$$

where we integrate only over members of the ensemble, omitting the Θ-function. Since the number of quadrons coincides in 2D with N_{DOF}, one can use the quadron volumes as the DOF when convenient

$$Z_v = \int e^{-\sum_{q=1}^{N\bar{z}} V^q/X}\, \omega\left(\{V^q\}\right) \Pi_{q=1}^{N\bar{z}} dV^q. \tag{5}$$

where $\omega\left(\{V^q\}\right)$ is an analogue of the density of states. In the ideal quadron gas approximation, i.e. assuming uncorrelated quadron volumes[3,24,25],

$$Z_v^{ig} = \left[\int e^{-V^q/X}\, \omega_1\left(V^q\right) dV^q\right]^{N\bar{z}} \tag{6}$$

where ω_1 is the one-quadron density of states [3]. While probably not accurate, the ideal quadron gas approximation simplifies (6), making possible exact analysis.

3 Construction of 2D dense packs of polydisperse discs

High packing fraction disc packs are achievable with Apollonian packing, for example, but these result in unrealistic structures with particular long-tailed disc size distributions. In most real system, the size and shape distributions, as well as maximal and minimal sizes, are given a-priori. To generate realistic high-density packs, we increase $\bar{z}$ by minimising the mean cell order, $\bar{z}_c$. Our construction is purely geometrical and does not enforce mechanical equilibrium.

Discs are deposited sequentially and the pack grows ad-infinitum, alleviating problems due to containing walls [23]. We start with a seed of three discs in contact, forming an order-3 cell. The discs radii are chosen from an initial uniform probability density function (PDF) between $1.0 = R^i_{\min} \leq R \leq R^i_{\max} = 2.0$. A new disc, chosen from the same PDF, is then attached to two of the existing discs. This process continues along the boundary of the growing pack. Adding a new disc n, its size is chosen from the uniform PDF and we try to attach it to two existing boundary discs already in contact – a and the previously added disc, b. If n does not overlap another already existing disc, the addition is accepted, generating an order-3 cell surrounded by a, b and n. If n overlaps a third disc c, we try to adjust n's size and location so that it is in contact with a, b and c. We limit the change of n's size to $\frac{1}{2}\min\{R_a, R_b, R_c\} \leq R_n \leq \frac{3}{2}R^i_{\max}$. If the resulting n is too small, R_b is reduced to allow more space for n. This latter step is repeated either until both n and b are acceptable or until no acceptable size can be achieved. In the latter case n is discarded and b's size and location are modified to fill the gap and contact c. If the increased R_b exceeds $\frac{3}{2}R^i_{\max}$, then the addition is cancelled and a new boundary pair a-b is chosen. The above steps eventually result in a modified disc n^*, be it n or b, touching three existing discs. Next, we check whether n^* overlaps with a fourth existing disc, d. If not, the addition is accepted. Otherwise we try to modify n^*'s size and location so that it contacts d and two of the three discs that it previously touched. This step fails if n^* is outside the size constraints, in which case n^* is discarded and new a and b are chosen.

Thus, the size constraints may force cells of order $z_c > 3$. This algorithm is very fast since the addition takes place at the pack boundary. Clusters of 10^6 discs can be generated within 20 s on an HP xw4600 Workstation (Intel Core 2 Quad 2.83 GHz 12 MB CPU, HP 8 GB(4×2 GB) DDR2-800 ECC Memory).

4 Results

Using the above protocol, we produced packs from 2000 to 5×10^5 discs (Fig. 2). Averaging over 1,200 packs of $N = 10^5$, we find a mean coordination number $\bar{z} = 5.217 \pm 0.004$ (referred to in the following, for brevity, as $\bar{z} = 5.2$) and a packing fraction $\phi = 0.870 \pm 0.006$. Unsurprisingly, this value is higher than of 2D random close packing of monodisperse discs, $\phi = 0.82$.

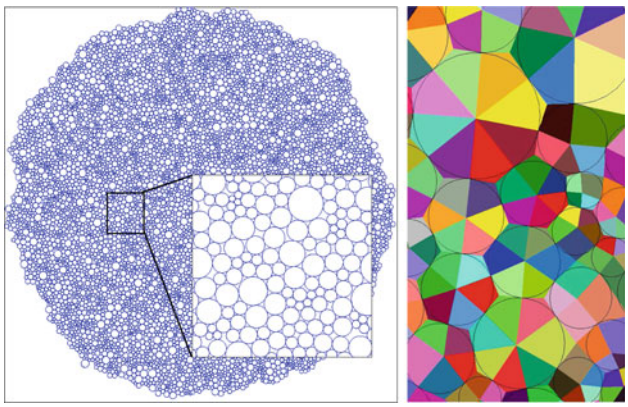

Fig. 2 *Left* A pack of 10^4 polydispere discs, produced by the algorithm described in Sect. 3. *Right* An example of the tessellation of the space by quadrons. Each quadron is shown in a different colour

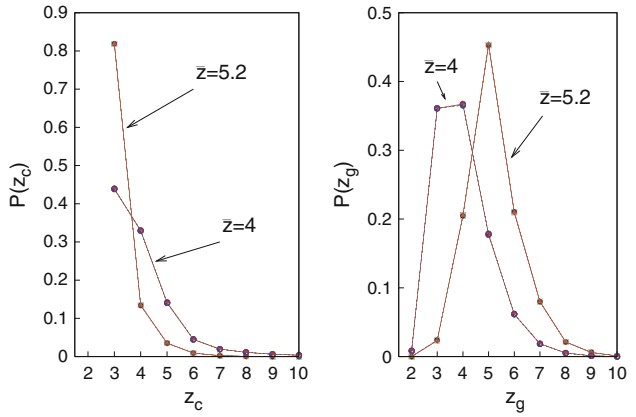

Fig. 3 The probabilities of (**a**) the cell order z_c and (**b**) the coordination number z_g for $\bar{z} = 5.2$ and $\bar{z} = 4$ for ten realisations of $N = 5 \times 10^5$

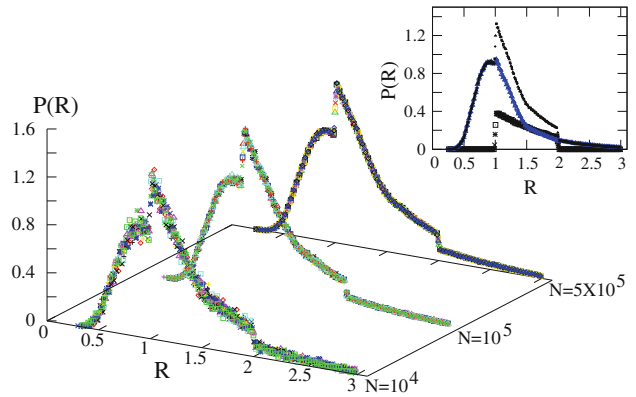

Fig. 4 The PDFs of disc radii for $N = 10^4, 10^5$ and 5×10^5 packs. Each plot is a superposition of ten realisations, showing that $N_{\text{lim}} \approx 10^5$. *Inset* the limit disc-size PDF (*black*) for 4 realisations of $N = 5 \times 10^5$ consists of a contribution from discs whose sizes were modified from the initial choice (*blue*) and from discs whose sizes were not (*black*) (Color figure online)

We expect the statistical mechanical formalism to apply to the limit statistics and we test emergence of such statistics against the following criteria: (i) all possible structural properties saturate to limit PDFs; (ii) the saturation occurs above an identifiable pack size N_{lim};(iii) different pack realisations saturate to the same limit statistics above N_{lim}.

As representative structural properties, we analysed the PDFs of z_g and z_c which saturate already for packs of $N \approx 1,000$. The collapse of PDFs of ten different packs is shown in Fig. 3 for $N = 5 \times 10^5$. The disc size PDF also converges to a limit form, which is distinctly different from the initial uniform one. The PDFs of ten different realisations, each for pack sizes $N = 10^4, 10^5$ and 5×10^5, are shown in Fig. 4. The figure shows that, for this quantity, $N_{\text{lim}} \approx 10^5$.

The limit disc size PDF can be understood as follows. The pack growth protocol allows controlled spillage outside the initial range $\left[R^i_{\text{min}} = 1, R^i_{\text{max}} = 2\right]$ to maximise the number of order-3 cells. This results in the seemingly discontinuous jumps at R^i_{min} and R^i_{max} (Fig. 4). Above R^i_{max} a tail evolved,

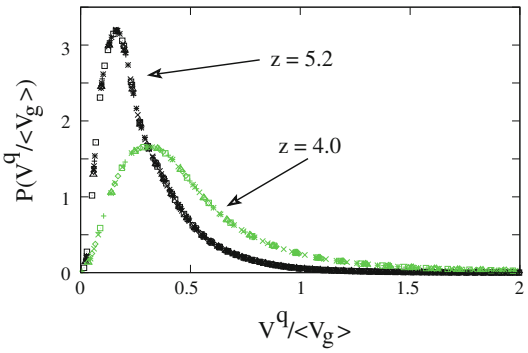

Fig. 5 The quadron volume PDFs of the dense pack with $\bar{z} = 5.2$ (*black*) and of the sparser pack with $\bar{z} = 4$ (*green*). The disc size distribution is the same for both packs. Plotted for each type of structure are the PDFs of ten realisations, which collapse nicely to one curve (Color figure online)

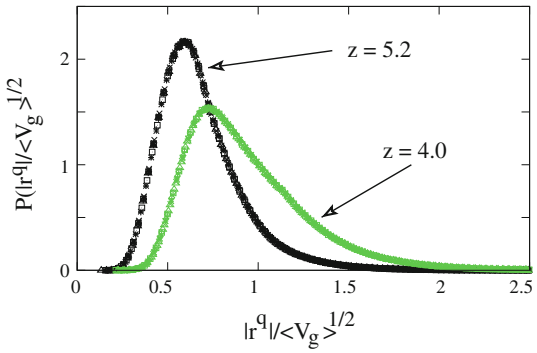

Fig. 6 The PDFs of $r^q = |\mathbf{r}^q|$ for the two different structures. The dense packs' PDF is in *black* and that of the sparser one, $\bar{z} = 4$, in *green*. Note the shift to higher values with the reduction of $\bar{z}$ due to the lower concentration of contact points (Color figure online)

cut off at $R^f_{\text{max}} = 3R^i_{\text{max}}/2$, while small size discs appear below R^i_{min}. Yet, in contrast to the monotonic decrease of the large-R tail, there develops a local maximum in the small-R regime. We cannot currently predict the functional form of the PDF in the three regimes. Nevertheless, the size PDF can be decomposed into two conditional PDFs: that of discs whose sizes were picked from the initial PDF and remained unchanged, and those whose sizes were modified as above (see inset in Fig. 4). The forms of these explains the origin of the discontinuous jumps.

The quadron statistics also converge to a limit form. In particular, their limit volume PDF, which underlies the statistical mechanical formalism, is shown in Fig. 5, for ten $N = 5 \times 10^5$ pack realisations.

As discussed above, identification and counting of the DOF are essential to the usefulness of the formalism. The DOF are a subset of $N\bar{z}/2$ of the 2D $\mathbf{r}^q$ vectors, giving $N_{\text{DOF}} = N\bar{z}$. The coincidence of this value with the number of quadrons allows using quadron volumes as the degrees of freedom. More generally, one needs the density of states $\omega(V^q)$. The systems are isotropic and therefore the orien-

tations of the $\mathbf{r}^q$ are uniformly distributed in $[0, 2\pi]$. The PDFs of their magnitudes $|\mathbf{r}^q|$ is shown in Fig. 6 from ten realisations.

The distribution of the quadron volumes is a product of the density of states and the Boltzmann-like factor and, in the ideal quadron gas model [3],

$$P(V^q) = \frac{1}{Z_v^{ig}(X)} e^{-V^q/X}\, \omega_1\big(V^q\big)\,. \tag{7}$$

To extract the density of states we need to examine ensembles of structures at different compactivities but the same density of states. Therefore, we have generated packs with $\bar{z} = 4$ and packing fraction $\phi = 0.80 \pm 0.01$, using the same disc size distribution (Fig. 4) and similar deposition procedure as for the $\bar{z} = 5.2$ packs. These packs are found to have only about half as many order-3 cells as the dense packs and many more cells of orders 4 and 5.

The probabilities of z_g and z_c for ten $N = 5 \times 10^5$ realisations in Fig. 3, shown alongside the dense packs for comparison, confirm emergence of limit statistics.

Similarly, we included the quadron volume PDF of the $\bar{z} = 4$ packs in Fig. 5 for comparison. We observe that lower $\bar{z}$ both shifts the PDF to higher volumes and broadens it. The former effect is not surprising since lower $\bar{z}$ leads to lower density and therefore to larger quadron volumes. The broadening is not as straightforward to understand, but we believe that it is caused by the broader PDF of z_c. Since our aim here is mainly to establish the utility of the method, we leave this study to a later report. We observe the same effects in the PDF of r^q, which we include in Fig. 6 for comparison with the dense packs.

Finally, from Eq. (7) we see that, from the ratio of two PDFs of structures with the same density of states, we can derive the difference between their inverse compactivities [26],

$$\ln\left\{\frac{P_{5.2}(V^q)}{P_4(V^q)}\right\} = -\left[\frac{1}{X_{5.2}} - \frac{1}{X_4}\right] V^q + \text{Const.} \tag{8}$$

An identical density of states is the consequence of the identical size distribution and similar pack growth procedure. We plot this ratio as a function of V^q in Fig. 7. The clear linear behaviour supports not only the assumption on the identical density of states but also the entire statistical mechanical approach. We find $\frac{1}{X_{5.2}} - \frac{1}{X_4} = 1.50 \pm 0.05$. The deviation from linearity at the very low volumes is due to the combination of finite packs and the overwhelming fraction of cells of order $z_c = 3$ in the dense packs. The deviation at the high volumes is due to the scarcity of high cell orders in the dense packs, leading to poor statistics in this range. Interestingly, the graph extrapolates to $(0, 0)$, the significance of which remains to be explored.

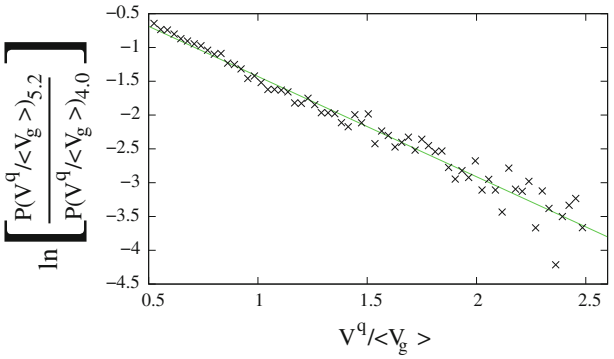

Fig. 7 The ratio of the quadron volume PDFs for statistics of the $\bar{z} = 5.2$ and $\bar{z} = 4$. For identical density of states, this ratio, Eq. (8), gives the difference between the inverse compactivities. The ratio is mainly exponential, giving $\frac{1}{X_{5.2}} - \frac{1}{X_4} = 1.5 \pm 0.05$

5 Conclusions

To conclude, we have used the Edwards statistical mechanics to report the following. (a)The development of a procedure to generate numerically dense 2D granular packs of polydisperse discs of bounded sizes. The procedure is very fast, making possible to generate packs of millions of discs on a desk workstation in under a minute. (b) The development of a similar procedure to generate packs of pre-determined disc size distributions, with mean coordination number $\bar{z} = 4$. (c) Demonstration that the dense and sparser packs converge to limit statistics for packs sizes of $N \lesssim 10^5$. (d) Computations and study of the probability functions of several structural quantities. Comparing two types of packs with the same disc size distribution and construction procedure, we have shown that the limit statistics are sensitive to $\bar{z}$. The quadron volume PDF peaks at lower values, which is expected, but it also narrows, which is less straightforward to understand. $\bar{z}$ had a similar effect on the distribution of the magnitudes of the vectors $\mathbf{r}^q$. (e) Analysis of the compactivities of the different pack types, showing that they have the same density of states and finding the difference between their inverse compactivities, $\frac{1}{X_{5.2}} - \frac{1}{X_4} = 1.50 \pm 0.05$.

These results provide a further step towards making the Edwards statistical mechanical formalism more applicable and useful. We expect that, once the compactivity is quantified for these systems, it will be possible to derive the density of states, using Eq. (7). This will then make it possible to obtain any structural property as an expectation value of the volume partition function Eq. (2).

Although different pack generation protocols should lead to different limit statistics and different limit disc size distribution, the methodology introduced here should work for any protocol. Our procedure of generating the two types of packs appears to leave the density of states unchanged and provides evidence for the exponential behaviour of the ratio of the PDFs of the quadron volumes.

We could only generate either very dense packs of $\bar{z} = 5.2$ or less dense ones of $\bar{z} = 4$. It would be interesting to generate packs with different values of $\bar{z}$ to complement this analysis and perhaps find the exact dependence of $X_{\bar{z}}$ on $\bar{z}$. We are currently studying this problem.

Acknowledgments This work was funded by Alan Howard Scholarship.

References

1. Ball, R.C., Blumenfeld, R.: Stress field in granular systems: loop forces and potential formulation. Phys. Rev. Lett. **88**, 115505 (2002)
2. Blumenfeld, R., Edwards, S.F.: Granular entropy: explicit calculations for planar assemblies. Phys. Rev. Lett. **90**, 114303 (2003)
3. Blumenfeld, R., Edwards, S.F.: Geometric partition functions of cellular systems: explicit calculation of the entropy in two and three dimensions. Euro. Phys. J. E **19**, 23 (2006)
4. Blumenfeld, R.: On entropic characterization of granular materials. In: Aste, T., Tordesillas, A., Matteo, T.D. (eds.) Lecture Notes in Complex Systems Vol. 8: Granular and Complex Materials, pp. 43–53. World Scientific (2008)
5. Edwards, S.F., Oakeshott, R.B.: The transmission of stress in an aggregate. Phys. D **38**, 88 (1989)
6. Edwards, S.F., Oakeshott, R.B.: Theory of powders. Phys. A **157**, 1080 (1989)
7. Mehta, A., Edwards, S.F.: Statistical mechanics of powder mixtures. Phys. A **157**, 1091 (1989)
8. Edwards, S.F.: The full canonical ensemble of a granular system. Phys. A **353**, 114 (2005)
9. Wittmer, J.P., Claudin, P., Cates, M.E., Bouchaud, J.-P.: An explanation for the central stress minimum in sand piles. Nature **382**, 336 (1996)
10. Wittmer, J.P., Cates, M.E., Claudin, P.: Stress propagation and arching in static sandpiles. J. Phys. I (France) **7**, 39 (1997)
11. Luding, S.: Stress distribution in static two-dimensional granular model media in the absence of friction. Phys. Rev. E **55**, 4720 (1997)
12. Cates, M.E., Wittmer, J.P., Bouchaud, J.-P., Claudin, P.: Jamming, force chains and fragile matter. Phys. Rev. Lett. **81**, 1841 (1998)
13. Edwards, S.F., Grinev, D.V.: Statistical mechanics of stress transmission in disordered granular arrays. Phys. Rev. Lett. **82**, 5397 (1999)
14. Vanel, L., Howell, D.W., Clark, D., Behringer, R.P., Clement, E.: Memories in sand: experimental tests of construction history on stress distributions under sandpiles. Phys. Rev. E **60**, R5040 (1999)
15. Silbert, L.E., Grest, G.S., Landry, J.W.: Statistics of the contact network in frictional and frictionless granular packings. Phys. Rev. E **66**, 061303 (2002)
16. Blumenfeld, R.: Stress transmission in planar disordered solid foams. J. Phys. A Math. Gen. **36**, 2399 (2003)
17. Blumenfeld, R.: Stresses in isostatic granular systems and emergence of force chains. Phys. Rev. Lett. **93**, 108301 (2004)
18. Snoeijer, J.H., Vlugt, T.J.H., van Hecke, M., van Saarloos, W.: Force network ensemble: a new approach to static granular matter. Phys. Rev. Lett. **92**, 054302 (2004)
19. Atman, A.P.F., Brunet, P., Geng, J., Reydellet, G., Claudin, P., Behringer, R.P., Clement, E.: From the stress response function (back) to the sand pile dip. Eur. Phys. J. E **17**, 93 (2005)
20. Ostojic, S., Somfai, E., Nienhuis, B.: Scale-invariance and universality of force networks in static granular matter. Nature **439**, 828 (2006)
21. Gerritsen, M., Kreiss, G., Blumenfeld, R.: Stress chain solutions in two-dimensional isostatic granular systems: fabric-dependent paths, leakage and branching. Phys. Rev. Lett. **101**, 098001 (2008)
22. Gerritsen, M., Kreiss, G., Blumenfeld, R.: Analysis of stresses in two-dimensional isostatic granular systems. Phys. A **387**, 6263–6276 (2008)
23. Desmond, K.W., Weeks, E.R.: Random close packing of disks and spheres in confined geometries. Phys. Rev. E **80**, 051305 (2009)
24. Frenkel, G., Blumenfeld, R., Grof, Z., King, P.R.: Structural characterization and statistical properties of two-dimensional granular systems. Phys. Rev. E **77**, 041304 (2008)
25. Frenkel, G., Blumenfeld, R., King, P.R., Blunt, M.J.: Topological analysis of foams and tetrahedral structures. Adv. Eng. Mater. **11**, 169–176 (2009)
26. McNamara, S., Richard, P., Kiesgen de Richter, S., Le Caer, G., Delannay, R.: Measurement of granular entropy. Phys. Rev. E **80**, 031301 (2009)